

HEAT TRANSFER AND FRICTION IN TUBES WITH REPEATED-RIB ROUGHNESS

R. L. WEBB

The Trane Company, La Crosse, Wisconsin, U.S.A.

E. R. G. ECKERT and R. J. GOLDSTEIN

University of Minnesota, Minneapolis, Minnesota, U.S.A.

(Received 12 March 1970 and in revised form 28 July 1970)

Abstract—Heat transfer and friction correlations are developed for turbulent flow in tubes having a repeated-rib roughness. The friction correlation is based on law of the wall similarity and is the same method employed by Nikuradse for sand-grain roughness. The heat transfer correlation is based on application of a heat-momentum transfer analogy to flow over a rough surface, which was first used by Dipprey and Sabersky for sand-grain roughness. The correlations are verified with experimental data taken with $0.01 < e/D < 0.04$ and $10 < p/e < 40$ and covering the range $0.71 < Pr < 37.6$. The correlations may be extended to a wider range of e/D by virtue of the law of the wall. The good results obtained in this study, supported by the prior work with sand-grain roughness, offer strong argument for application of the correlating methods to other roughness geometries. The success of the heat-momentum analogy correlation is compared with other methods frequently found in the literature.

NOMENCLATURE

<p>D, pipe inside diameter (to base of ribs);</p> <p>D_{eq}, equivalent diameter $D_{eq} \equiv D - e$;</p> <p>D'_{eq}, defined by Hall [12];</p> <p>e, height of roughness element;</p> <p>e_{sg}, equivalent sand-grain roughness, $\ln(e_{sg}/e) = (8.48 - u_e^+)/2.5$;</p> <p>$e^+$, $e^+ \equiv eu^*/\nu = (e/D)Re\sqrt{f/2}$;</p> <p>$e_{sg}^+$, $e_{sg}^+ \equiv e_{sg}u^*/\nu$;</p> <p>$f$, friction factor, $f \equiv (\Delta P/L)D/2u_m^2$;</p> <p>$F(Pr)$, Prandtl number function, cf. equations (14) and (18a);</p> <p>g, $g \equiv (f/2St - 1)\sqrt{(f/2) + u_e^+}$;</p> <p>$\bar{g}$, $\bar{g} \equiv gPr^{-n}$ ($n = 0.57$ for repeated-ribs);</p> <p>p, distance between repeated-ribs;</p> <p>Pr, Prandtl number, evaluated at T_{av};</p> <p>Pr_e, effective Prandtl number, $Pr_e \equiv \nu_e/\alpha_e$;</p> <p>$q$, heat flux;</p> <p>$R$, pipe radius;</p> <p>$Re$, Reynolds number $Re \equiv Du_m/\nu$;</p> <p>St, Stanton number;</p> <p>T_{av}, mixed mean fluid temperature;</p>	<p>T^+, dimensionless temperature, $T^+ \equiv T/(q_w/\rho c_p u^*)$;</p> <p>$u$, local fluid velocity;</p> <p>u_c, velocity at pipe centerline;</p> <p>u_m, average fluid velocity;</p> <p>u^+, dimensionless velocity, $u^+ \equiv u/u^*$;</p> <p>u_e^+, $u_e^+ \equiv \sqrt{(2/f) + 2.5 \ln(2e/D) + 3.75}$;</p> <p>$\bar{u}_e^+$, $\bar{u}_e^+ \equiv \sqrt{(2/f) + 2.5 \ln(2e_{sg}/D) + 3.75}$;</p> <p>$u^*$, "friction velocity," $u^* \equiv \sqrt{(\tau_o/\rho)}$;</p> <p>$y$, coordinate distance normal to wall;</p> <p>y_b, thickness of viscous influenced region;</p> <p>y^+, dimensionless distance, $y^+ \equiv yu^*/\nu$;</p> <p>y_m, distance from wall at which $u = u_m$.</p> <p style="text-align: center;">Greek symbols</p> <p>α, thermal diffusivity, $\alpha \equiv k/\rho c$;</p> <p>α_e, effective diffusivity, $\alpha_e \equiv \alpha + \epsilon_h$;</p> <p>$\epsilon_h$, eddy diffusivity of heat;</p> <p>ϵ_m, eddy diffusivity of momentum;</p> <p>η, efficiency index, $\eta \equiv (St/St_s)/(f/f_s)$;</p> <p>$\phi$, general functional specification;</p> <p>ν, kinematic viscosity;</p>
--	--

ν_e ,	effective kinematic viscosity, $\nu_e \equiv \nu + \varepsilon_m$;
τ ,	local time average shear stress;
τ_0 ,	apparent wall shear stress, $\tau_0 \equiv -(D/4)dP/dX$;
τ_w ,	wall shear stress.

Subscripts

m ,	evaluated at $y = y_m$;
s ,	smooth tube;
w ,	evaluated at wall.

Unsubscripted f , St , $F(Pr)$ refer to rough tube.

INTRODUCTION

THIS study seeks to develop a generalized understanding of the Stanton number and friction characteristics of "repeated-rib" roughness in turbulent pipe flow. The roughness geometry is shown in Fig. 1 and is described by the

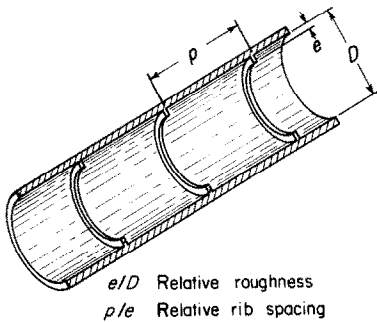


FIG. 1. Characteristic dimensions of repeated-rib roughness.

dimensionless parameters e/D and p/e , assuming that the rib thickness is small, relative to the rib spacing. This understanding will permit pre-

diction of the friction factor as a function of the variables e/D , p/e and Re . The Stanton number is described as a function of the same variables, plus the Prandtl number.

A number of heat-transfer measurements have been performed for repeated-rib roughness in pipe flow, as shown in Table 1. This body of work has not resulted in a rationally based correlation for the St and f as a function of the geometric variables (e/D , p/e) and Prandtl number. Most of the data were taken in the fully rough region (where f is independent of Re) resulting in an incomplete understanding of the heat transfer characteristics in the transition region before the fully rough condition is attained. In addition, most of the work was done with air flow so the Prandtl number influence is not well established. Those who have studied the effect of Prandtl number in rough tubes offer conflicting results. Gomelaui [9], who worked with an annular flow, and Kalinan [7] indicate that the Prandtl number dependency of repeated-rib roughness and smooth tubes is approximately equal. However, Kolar [10] and Burck [11] used a screw-thread type roughness ($p/e \approx 2$) in pipe flow and found that the heat transfer augmentation, St/St_s for a given roughness, increases with increasing Prandtl number.

Considerable data exist for repeated-rib roughness in an annular flow geometry in which the inner annulus surface is rough and the outer surface is smooth. The hydraulic diameter reasonably correlates smooth annular flow friction data with pipe data, but the concept does

Table 1. Data for repeated-rib roughness in circular tubes (T-transverse ribs; H-rib in helical form)

Ref	Author	Rib type	e/D	p/e	$Re \times 10^{-3}$	Pr	
[1]	Nunner		T	0.04-0.08	2-81.7	1-100	0.7
[2]	Koch		T	0.04-0.25	4-200	1-100	0.7
[3]	Gargaud <i>et al.</i>		H, T	0.0004-0.016	1.1-15	200-3000	0.7
[4]	Molloy		H	0.014	10	2-70	0.7
[5]	Sutherland <i>et al.</i>		H	0.0035	11.8	10-400	1.0
[6]	Brouillette <i>et al.</i>		H	0.005-0.10	5-14	30-150	water
[7]	Kalinin <i>et al.</i>		T	0.015-0.05	20-100	10-140	0.7-50
[8]	Sams		H	0.008-0.02	1.0	5-300	0.7
—	This study		T	0.01-0.04	10-40	6-100	0.7-38

not hold when only one surface of the annulus is roughened. An equivalent diameter, D'_{eq} has been proposed by Hall [12], who theorizes that annulus data based on the derived e/D'_{eq} should agree with the results obtained in pipe flow for geometrically similar roughness if $e/D'_{eq} = e/D$.

Although the repeated-rib surface may be considered as a "roughness" geometry, it may also be viewed as a problem in boundary layer separation and reattachment. Figure 2 shows a

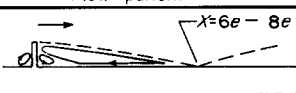

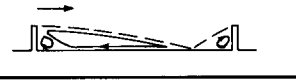
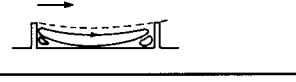
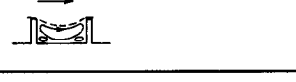

Ref	p/e	Flow pattern
[15]	$\rightarrow \infty$	
[16]	10	
[16]	8	
[16] [17]	5	
[16] [17]	2	
[16] [18]	0.75- 1.25	

FIG. 2. Flow patterns as a function of p/e .

catalog of flow patterns downstream from a rib, as a function of the relative rib spacing (p/e). Separation occurs at the rib, forming a widening free shear layer which reattaches 6–8 rib heights downstream from the separation point. A reverse flow boundary layer originates at the reattachment point and grows in thickness in the upstream region. The boundary layer tends toward redevelopment downstream from the reattachment point. The wall shear stress is zero at the reattachment point and increases from zero in the reverse flow and reattachment regions; however, the direction of the shear stress is opposite in these regions. Reattachment does not occur for p/e less than about eight.

Measurements of the local heat-transfer coefficient downstream from the rib [13, 14] show that a maximum heat-transfer coefficient occurs in the vicinity of the reattachment point. The local heat-transfer coefficients in the separated flow region are larger than those of an undisturbed boundary layer, although this is not true for laminar flow downstream from a rib.

Friction correlation

A friction correlation for flow over "sand-grain" roughness was developed by Nikuradse [19]. Based on law of the wall similarity, Nikuradse found that his data, covering a wide range of e/D , was correlated by the friction similarity function†

$$u_e^+(e^+) \equiv \sqrt{(2/f) + 2.5 \ln(2e/D) + 3.75}$$

where e^+ is the "roughness Reynolds number". If law of the wall similarity is assumed applicable to arbitrary types of roughness, the same parameters should correlate the friction data for any geometrically similar roughness family.‡ A generalized friction correlation for the repeated-rib roughness, which accounts for both roughness parameters (e/D and p/e), has not been established.

Heat transfer correlation

Nunner [1] was the first to propose a flow model. He proposed that the roughness acts to reduce the thermal resistance of the turbulence dominated wall region without significantly affecting the viscous region. He likened this to the temperature profile in smooth tube flow at increased Prandtl number. The argument was quantified by using the Prandtl analogy and replacing Pr by $(f/f_s)Pr$. This model predicts decreasing St/St_s with increased Prandtl number, contrary to the previously discussed results.

† The function $u_e^+(e^+)$ used here is equivalent to the symbol $B(e^+)$ used by Nikuradse. In the "fully rough" condition ($e^+ > 70$), $B(e^+) = 8.48$.

‡ A family of repeated-rib roughness is defined as geometrically similar if $p/e = \text{constant}$ and the rib shape is not varied.

Further, it predicts that St/St_s is independent of the roughness type.

Assuming that law of the wall similarity applies to the temperature profile as well as to the velocity profile, Dipprey and Sabersky [20] developed a heat-momentum transfer analogy relation for flow in a sand-grain roughened tube. They achieved excellent correlation of their data using the correlation

$$(f/2St - 1)/\sqrt{(f/2) + 8.48} = g(e^+, Pr).$$

They assumed that their roughness closely approximated that used by Nikuradse and calculated e^+ in terms of the Nikuradse sand-grain roughness, using $u_e^+ = 8.48$. The concept proposed by Dipprey and Sabersky is so general it may apply to any roughness for which law of the wall similarity holds. Sheriff and Gumley [21] applied the concept to their repeated-rib annulus air flow data using a friction factor defined in terms of D_{eq} and likewise achieved good correlation.

Sutherland [22] and Sheriff and Gumley [21] have found that the empirical correlation St/St_s vs. e^+ worked as well as the Dipprey and Sabersky model for air flow over repeated-ribs with $p/e = 10$.

Using data for several basic types of non-geometrically similar roughnesses (repeated-rib, sand-grain and screw-threads), Burck [11] concluded that the heat-transfer data of *all* roughness geometries may be correlated in the form $\eta(e_{sg}^+, Pr)$, where e_{sg}^+ is the equivalent Nikuradse sand-grain roughness. Thus, Burck concludes that all roughness types yield the same performance (e.g. the same η) if evaluated at equal e_{sg}^+ .

It should be noted that none of the correlations can be reduced to yield equivalent algebraic expressions.

ANALYSIS

The flow over a rough surface is not sufficiently understood to permit heat transfer and friction prediction by analytical methods nor is there even general agreement on the parameters

which should be used to correlate the data. Law of the wall similarity is, however, a reasonably well accepted concept, and a friction correlation based on this concept seems warranted. Due to the good results achieved by Dipprey and Sabersky, the heat-momentum transfer analogy, based on law of the wall similarity, offers promise of application to other types of geometrically similar roughnesses. These concepts will be developed and applied to correlation of the repeated-rib data.

The rough surface analysis employs essentially the same concepts, which are commonly accepted in analysis of flow over smooth surfaces, although certain assumptions are different. Parallel analyses will be shown for the rough and smooth surface cases in order to show the similarities and differences of the two cases. The rough surface analysis is developed for an arbitrary roughness geometry whose characteristic dimension is e/D . Subsequently, the results are extended to include the p/e dimension.

Momentum transfer analysis

Measured velocity distributions show that the effects of viscosity and surface roughness differ in the inner and outer regions of the turbulent boundary layer. In the outer region the velocity defect, $(u_c - u)/u^*$, is insensitive to viscosity and roughness. This "velocity defect law" is described by equations (1a) and (1b) in Table 2. In contrast the velocity near the wall is sensitive, both to viscosity and the type of roughness; this phenomenon is termed "law of the wall" similarity and is described by equations (2a) and (2b) of Table 2. Law of the wall similarity implies that the wall region velocity distribution for geometrically similar roughness depends only on e^+ and is independent of the pipe Reynolds number. Based on a detailed re-evaluation of velocity distribution measurements in smooth and rough pipes, Hinze [31] concludes that these velocity distribution laws do not appear to be strictly independent of pipe Reynolds number, and so they should be regarded as good approximations. Assuming a region of overlap

(a region in which either law adequately predicts the velocity in at least a small region $\Delta y/R$), the law of the wall and the velocity defect law are combined to give algebraic equations for the turbulence dominated part of the wall region [equations (3a) and (3b)]; the constants are those proposed by Nikuradse [18]. The smooth surface equation holds beyond $y^+ \simeq 26$ from the surface, and the rough surface equation is not expected to hold for $y < e$. Equations (3a) and (3b) are frequently assumed to hold up to the pipe centerline, although this is an approximation. Assuming that equations (3a) and (3b) hold

pipe flow following a somewhat different derivation than that used by Dipprey and Sabersky. The development assumes that the heat and momentum transport equations of fully developed flow can be approximately applied to the flow in a rough pipe. The assumption should be reasonable in the region $y > e$ with small e/D . In the region $y < e$, where radial velocities exist, one may postulate that the concept involves the equivalent fully developed transport equations of the spatially averaged periodic flow.

With flow in a smooth tube, the only forces in the axial direction are the static pressure

Table 2. Velocity distribution and friction expressions

Smooth tube		Rough tube	
$(u_c - u)/u^* = \phi_1(y/R)$	(1a)	$(u_c - u)/u^* = \phi_1(y/R)$	(1b)
$u/u^* = \phi_2(yu^*/v)$	(2a)	$u/u^* = \phi_3(y/e) + \phi_4(eu^*/v)$	(2b)
$u/u^* = 2.5 \ln(yu^*/v) + 5.5$	(3a)	$u/u^* = 2.5 \ln(y/e) + u_e^+(e^+)$	(3b)
$\sqrt{(2/f)} = 2.5 \ln(Du^*/2v) + 1.75$	(4a)	$\sqrt{(2/f)} = 2.5 \ln(D/2e) + u_e^+(e^+) - 3.75$	(4b)

approximately over the entire cross-section, the friction factor is given by the integrated velocity distribution, equations (4a) and (4b). Equation (4b) defines the friction similarity law for rough surfaces; thus, u_e^+ vs. e^+ should correlate all friction data for any type of geometrically similar roughnesses. According to equation (3b), u_e^+ is the average dimensionless velocity at $y = e$. In the fully rough condition u_e^+ attains a constant value, which implies that the wall region velocity distribution is not affected by the fluid viscosity, and that any viscosity effects are confined within $y < e$. Equation (3b) shows that u_e^+ should be independent of tube diameter for geometrically similar roughness. Nikuradse found this to be true for sand-grain roughness in fixed diameter tubes whose e/D varied as much as 16:1. It is reasonable to expect the same result for the repeated-rib roughness, although u_e^+ will be a function of p/e as well as of e^+ .

The heat-momentum transfer analogy is developed for a turbulent, Newtonian fluid in

gradient and the fluid shear stress; as a consequence, a linear shear stress distribution exists.

$$-\frac{1}{2\rho} \frac{dP}{dx} = \frac{\tau}{(R-y)} = \frac{\tau_w}{R}. \quad (5)$$

Equation (5) is commonly applied to flow in rough tubes by replacing the wall shear stress (τ_w) by τ_0 , which arbitrarily assigns the effect of all drag forces to the wall. Thus for the rough surface,

$$-\frac{1}{2\rho} \frac{dP}{dx} = \frac{\tau}{(R-y)} = \frac{\tau_0}{R}. \quad (6)$$

Equation (6) should well approximate the shear stress distribution for $y > e$ but not in the roughness region ($y < e$) where pressure forces act on the roughness elements. Figure 3 illustrates the radial distribution of the stream-wise averaged shear stress using equation (6) only for the region $y > e$. Figure 3 proposes that the shear stress distribution in the region $y < e$ is significantly different from that which exists in smooth tubes.

subtracted to make use of equation (11).

$$\frac{\sqrt{(f_s/2)}}{St_s} = \int_0^{y_b^+} (Pr_\varepsilon - 1) \frac{du^+}{dy^+} dy^+ + \int_0^{y_m^+} \frac{du^+}{dy^+} dy^+. \quad (12)$$

The second integral, defined by equation (11), is combined with the left-hand side of equation (12) to give

$$\frac{f_s/2St_s - 1}{\sqrt{(f_s/2)}} = \int_0^{y_b^+} (Pr_\varepsilon - 1) \frac{du^+}{dy^+} dy^+. \quad (13)$$

The upper limit of the integral in equation (13) is a constant ($y_b^+ \approx 26$), and the velocity distribution is defined by the law of the wall [equation (3a)], which is assumed to be independent of the Reynolds number. Experimental information indicates that the Reynolds number has an insignificant effect on Pr_ε when liquid metals are excluded [24]. Neglecting the slight Reynolds number dependency, the integral in equation (13) is a function only of Pr , i.e. $F_s(Pr)$. Several formulations for $F_s(Pr)$ are given in the literature, e.g. the Prandtl and von Kármán analogy formulations. The widely accepted numerical solutions of Deissler [25] and Sparrow *et al.* [26] are well approximated, especially for $Pr > 1$, by the empirical equation

$$F_s(Pr) = 9.3 (Pr - 1) Pr^{-1/4}. \quad (14)$$

Substitution of equation (14) in equation (13) and solving for the smooth tube Stanton number,

$$St_s = \frac{f_s/2}{1 + 9.3\sqrt{(f_s/2)}(Pr - 1)Pr^{-1/4}}. \quad (15)$$

The integration of equation (9) for flow in a rough tube, whose characteristic roughness is e/D , follows a similar procedure. The integrals are again written over the viscous and turbulence dominated regions, and terms are added and subtracted to make use of the identities. Using

the rough surface assumptions of Table 3, the initial integral formulation is

$$\frac{\sqrt{(f/2)}}{St} = \int_0^{e^+} \frac{q}{q_w} \frac{\tau_0}{\tau} Pr_\varepsilon \frac{du^+}{dy^+} dy^+ + \int_{e^+}^{y_b^+} (Pr_\varepsilon - 1) \frac{du^+}{dy^+} dy^+ + \int_{e^+}^{y_m^+} \frac{du^+}{dy^+} dy^+. \quad (16)$$

Equation (16) includes the possibility that y_b may be less or greater than the roughness height, e ; the second integral drops out if $y_b < e$. The third integral can be written as $[\sqrt{(2/f)} - u_e^+]$, and equation (16) reduces to [c.f. equation (13)]:

$$\frac{f/2St - 1}{\sqrt{(f/2)}} + u_e^+ = \int_0^{e^+} \frac{q}{q_w} \frac{\tau_0}{\tau} Pr_\varepsilon \frac{du^+}{dy^+} dy^+ + \int_{e^+}^{y_m^+} (Pr_\varepsilon - 1) \frac{du^+}{dy^+} dy^+. \quad (17)$$

Assuming f is known, e^+ may be calculated, and u_e^+ is given by equation (4b). The rough surface Stanton number could be computed if the other variables in equation (17) were known. This is precisely where fundamental knowledge of flow over rough surfaces is lacking. Even the detailed work of Nikuradse cannot be utilized to determine the velocity distribution in the roughness region $y < e$. However, if the integrands in equation (17) can be defined as functions of known variables, the equation will define the parameters necessary to correlate the rough surface heat transfer data. The variable y_b^+ is not a constant, as for a smooth surface. By law of the wall similarity, y_b^+ is a function of e^+ , and the variables τ/τ_0 and u^+ are implicitly defined for geometrically similar roughness. Assuming that the effect of Re on Pr_ε is negligible, Pr_ε is a function of Pr for geometrically similar roughnesses.

Dipprey and Sabersky proposed that law of the wall similarity also applies to the temperature distribution in rough tubes, thus implicitly defining the variable q/q_w . Because equation

(17) requires evaluation of q/q_w only over the very small interval, $0 < y < e$, one may just as well propose $q/q_w \approx 1$, or alternatively $q/q_w = (1 - y/R)$, which is usually assumed for flow in smooth tubes. In either case, no new functional arguments are specified. By this reasoning, equation (17) is written in the functional form

$$(f/2St - 1)/\sqrt{(f/2)} + u_e^+ = \phi_5(e^+, Pr) + \phi_6(e^+, Pr) \equiv g(e^+, Pr). \quad (18)$$

If the Prandtl number dependency of equation (18) can be separated,

$$(f/2St - 1)/\sqrt{(f/2)} + u_e^+ = \bar{g}(e^+) F(Pr). \quad (18a)$$

Equation (18a) defines the correlating parameters for any geometrically similar roughness whose characteristic roughness dimension is e/D . Repeated-rib roughness is geometrically similar if $p/e = \text{constant}$. To account for variation of p/e with the repeated-rib roughness, equation (18a) is modified to

$$(f/2St - 1)/\sqrt{(f/2)} + u_e^+ = \bar{g}(e^+, p/e) F(Pr). \quad (18b)$$

EXPERIMENTAL PROGRAM

Experimental data were taken with circular tubes having repeated-rib roughness to test the correlating equations over a wide range of roughness dimensions, Reynolds number and Prandtl number. Five rough tube and one smooth tube sections were constructed. Table 4 gives the dimensionless roughness parameters

Table 4. Test section description

Tube	e/D	p/e
01/10	0.01	10
02/10	0.02	10
04/10	0.04	10
02/20	0.02	20
02/40	0.02	40

and defines a reference code for each of the rough tubes.

The first three test sections have geometrically similar roughness (defined within the concept

of law of the wall similarity), and the second plus the last two were constructed to determine the effect of p/e . Data were taken on each test section at three Prandtl numbers (0.71, 5.10 and 21.7) with $6000 < Re < 100000$. The Prandtl number range was obtained using three fluids: air, water and n-butyl alcohol. Several of the tubes were also tested with butyl alcohol at $Pr = 37.6$ for which the maximum Reynolds number was limited to 42000.

Each rough tube test section consisted of two identical copper tubes having $D = 36.83$ mm (1.45 in.) by 152.4 cm (60 in.) long. The first tube served as an unheated hydraulic entry section, and the second was electrically heated and used for heat transfer measurements. The repeated-rib test sections were fabricated by first machining a number of pipe segments of length p , each having a transverse rib, 0.38 mm (0.015 in.) thick and height e . The tolerance on all machined dimensions was within 0.040 mm. The segments were stacked and brazed to form the full length test sections. The brazing alloy was prevented from flowing on the inner tube surface. The brazed pipes were installed in a lathe and turned down to 41.28 mm (1.625 in.) o.d. and then cleaned. Two sets of five thermocouples, circumferentially separated 180°, were installed in 0.30 mm square grooves machined in the tube outer circumference. Nichrome ribbon, 31.8 mm \times 0.081 mm, was wrapped in a helix on the heat-transfer tube. The Nichrome ribbon was electrically insulated by 0.10 mm thick adhesive backed Teflon tape, cemented to the heating ribbon.

For operation with liquids, a pump supplied liquid to a water-cooled heat exchanger. The liquid then flowed thru the test section and back to the pump suction which was maintained at 1.7 bars (25 psig). Operation with air flow was accomplished by introducing compressed air through a pressure regulator into the orifice section and subsequently exhausting it into the atmosphere downstream from the test section. Test section heat input was provided by auto-transformer controlled power supplies and

measured by precision wattmeters. All wetted surfaces were made from copper or stainless steel to minimize corrosion and fouling.

Figure 4 shows the measuring section, consisting of a smooth entry section, the rough hydraulic entry and heat transfer test sections

local variation of the inner wall temperature. The degree to which the copper test section achieved this condition was determined by numerical solution of the heat conduction equation using an approximation of the expected local heat-transfer coefficient distribution. The

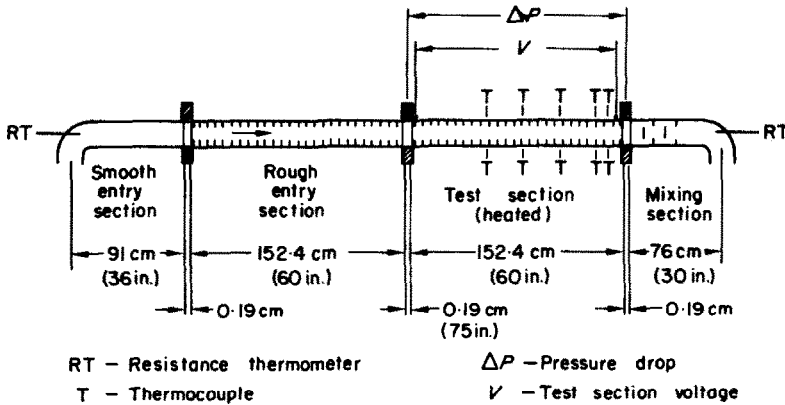


FIG. 4. Sketch of instrumented measuring section.

and a mixing section. The entire measuring section was thermally insulated by a surrounding duct filled with Silica Aerogel. Nylon bushings, 19 mm (0.75 in.) thick, bored to the base diameter of the pipe, were precisely installed between mating test section flanges. The test section pressure drop was measured between pressure taps drilled in the Nylon bushings. The measuring section inlet and exit fluid temperatures were measured by resistance thermometers, and the test section pressure drop with U-tube or travelling well micromanometers. The wall thermocouple millivolt output was read on a precision potentiometer. A more complete description of the apparatus is given by Webb [27].

The local heat-transfer coefficient varies about 35 per cent from its peak value at the re-attachment point to the rib location [14]. By using a thick walled, high conductivity tube, a constant heat flux applied to the tube external surface will very nearly redistribute within the tube wall, matching the local heat-transfer coefficient distribution, resulting in a negligible

calculated local temperature difference (between the outer wall and the fluid temperature) differed about 1 per cent along the distance between ribs.

The friction factors were determined with air as the working fluid and without heat input. They are based on the pressure drop over a 152.4 cm tube length, preceded by a 91 cm smooth and a 152.4 cm rough development length. The measured pressure loss was corrected to account for the length of the smooth Nylon bushings; the maximum correction applied was only one per cent. The Prandtl number variation, based on the average fluid temperature, was held within ± 0.40 per cent. In order to minimize the effect of fluid property variation in the wall region, the test section power input was selected to give $Pr/Pr_w \approx 1.1$ in the liquid tests. Two additional, higher heat flux runs were taken with the butyl alcohol at $Re \approx 30000$ to determine the degree to which the heat-transfer coefficients differed from the constant property fluid condition. The property ratio exponent, based on the Prandtl number, was found to be

larger than observed for smooth tubes, 0.25 vs. 0.15. The rough tube liquid flow heat-transfer data were not corrected to the constant property condition, since the correction would reduce the Stanton numbers only 2-3 per cent. The heat-transfer coefficient of the rough tubes is defined in terms of the base area of the 36.83 mm i.d. tube and does not include the surface area increase due to the ribs.

RESULTS AND DISCUSSION

Figure 5 shows the results for the smooth tube. The friction factor agrees well with equation (4a), shown on Fig. 5. The smooth

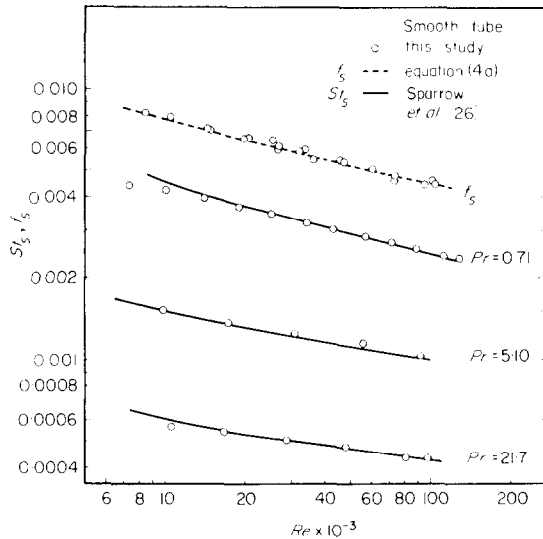


FIG. 5. Smooth tube heat transfer and friction data.

tube Stanton numbers are corrected to the constant property condition, multiplying St_s by the factor $(Pr/Pr_w)^{-0.11}$ as recommended by Hufschmidt *et al.* [28]; the correction amounted to less than 2 per cent. The solid lines on Fig. 5 are the constant property Stanton number predictions of the Sparrow *et al.* analytical solution [26]. The experimental data agree well with the analytical solution for $Re > 10000$.

The rough tube data are shown in Figs. 6 and 7. Figure 6 shows the data for the geometrically

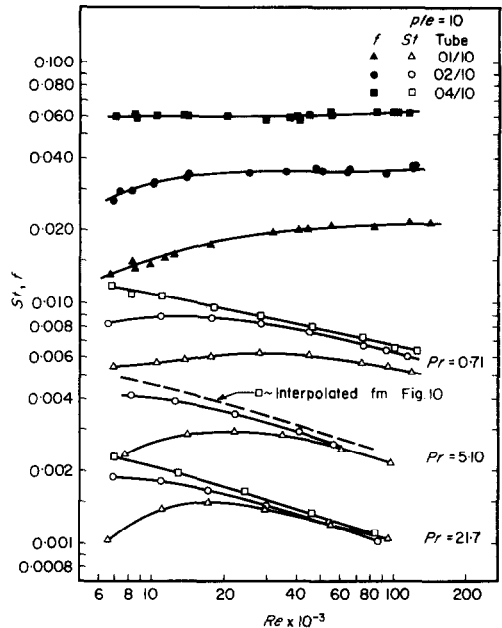


FIG. 6. Repeated-rib heat transfer and friction data for geometrically similar roughness ($p/e = 10$).

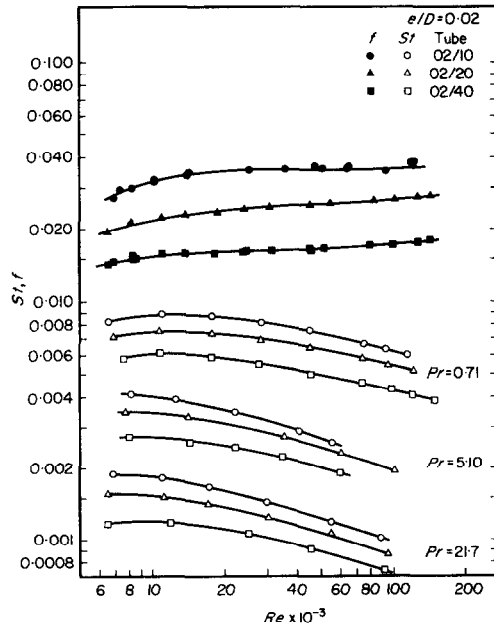


FIG. 7. Repeated-rib heat transfer and friction data for non-geometrically similar roughness, $e/D = 0.02$.

similar roughness ($p/e = 10$), and Fig. 7 shows the effect of varying p/e , with $e/D = 0.02$. In the "fully rough" condition, the friction factors supposedly attain a constant value, independent of Reynolds number. These data show a small positive slope for $Re > 100000$. This may be attributed to the very small scale roughness left by the lathe cutting tool; this roughness was judged to have $e/D \approx 3 \times 10^{-5}$. The Stanton number data, except for the roughest tube (04/10), either show or suggest a maximum Stanton number. The Reynolds number at which this maximum occurs decreases slightly as the Prandtl number is increased. The maximum Stanton number for $Pr = 0.71$ appears to be attained just before the fully rough condition is reached.

Correlation of friction data

Correlation of the rough tube friction data is shown on Fig. 8. The data for the non-geometrically similar roughnesses are displaced,

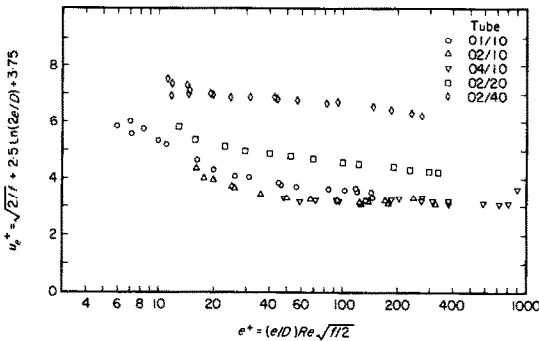


FIG. 8. Friction correlating parameter u_e^+ vs. e^+ .

as expected, due to their different values of p/e . The proposed e/D independence for geometrically similar roughness is evaluated by comparing the data for tubes 01/10, 02/10 and 04/10. The correlation for 02/10 and 04/10 is excellent; however, the u_e^+ for 01/10 is about 12 per cent greater. The 01/10 friction factor is about 7 per cent smaller than would be predicted from the value of u_e^+ for tubes 02/10 and 04/10.

The dependence of u_e^+ on p/e was determined by cross-plotting u_e^+ vs. e^+ on logarithmic coordinates, and the results are shown on Fig. 9. The simple dependence, $(p/e)^{-0.53}$, correlates the data for $e^+ > 35$, and in the fully rough region $u_e^+ = 0.95 (p/e)^{0.53}$.

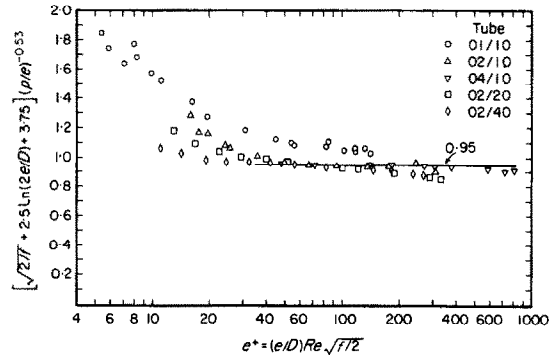


FIG. 9. Final friction correlation for repeated-rib tubes.

There are several possible explanations for the slightly larger than anticipated values of u_e^+ for the 01/10 tube, relative to that for tubes 02/10 and 04/10. The three tubes have the same rib thickness so their roughnesses are not precisely geometrically similar. Geometric roughness similarity also requires that all radii, fillets, etc., be shrunk in the same proportion; this condition was not met in the machining operation. A more probable possibility involves the definition of an equivalent diameter. The base surface is seldom taken as the origin for the velocity distribution measurements with rough surfaces. For example, Betterman [29] set the origin at $y = 0.6e - 0.8e$ above the base surface in his velocity measurements with rough surfaces; this yielded a linear velocity distribution on logarithmic coordinates. The scatter of the correlated friction data (corresponding to Fig. 9) is reduced to about ± 6.0 per cent using f and Re defined by the equivalent diameter $D_{eq} \equiv D - e$.

Correlation of the heat-transfer data

The heat-transfer data correlated in the

functional form of equation (18b) are shown on Fig. 10 for each of the four Prandtl numbers. No significant dependence of g on p/e is observed

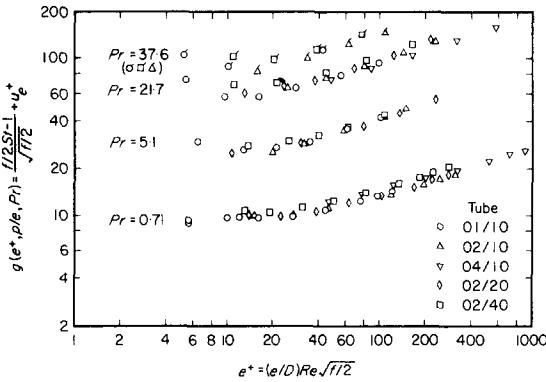


FIG. 10. Heat-transfer correlations, $g(e^+, p/e, Pr)$ vs. e^+ for four Prandtl numbers.

except possibly for $Pr > 21.7$ with $e^+ < 35$. In this region the data for $p/e = 40$ are about 15 per cent above the other data. Figure 10 indicates that g attains a minimum value at $e^+ \approx 12$ for $Pr \geq 5.1$; however, a minimum is not obvious for $Pr = 0.71$.

A cross-plot of g vs. Pr gives $g \propto Pr^{0.57}$. The final heat transfer correlation is shown on Fig. 11

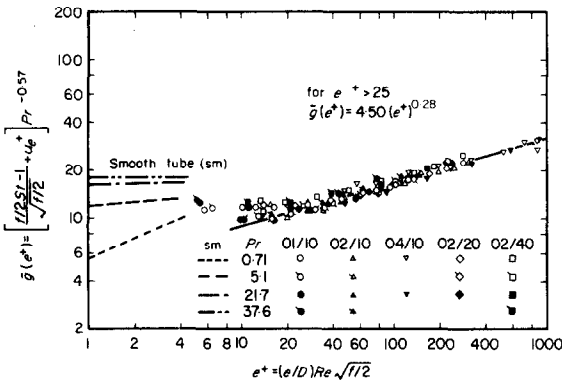


FIG. 11. Final heat transfer correlation, $\bar{g}(e^+)$ vs. e^+ including the Prandtl number dependency.

as $\bar{g}(e^+)$ vs. e^+ . The small effect of p/e on the heat-transfer correlation is not considered significant for engineering purposes and is not included as an argument of the function \bar{g} . The

Prandtl number function for repeated-rib roughness [c.f. equation (18b)] is $F(Pr) = Pr^{-0.57}$, which is different from $F(Pr) = Pr^{-0.44}$ found by Dipprey and Sabersky for sand-grain roughness.

The heat transfer and friction characteristics are expected to approach a hydraulically smooth condition at some small value of e^+ . The dashed lines near the left-hand side of Fig. 11 show the curves of

$$[(f_s/2St_s - 1)/\sqrt{(f_s/2)} + u_e^+] Pr^{-0.57}$$

predicted for hydraulically smooth tubes; $(f_s/2St_s - 1)/\sqrt{(f_s/2)}$ is given by equation (14) and $u_e^+ = 2.5 \ln e^+ + 5.5$ is obtained using the friction factor from equation (4a) in equation (4b). The relative separation of these dashed lines indicates a Prandtl number dependency different from $g \propto Pr^{0.57}$ as the hydraulically smooth condition is approached.

An equation for the Stanton number is formulated from equation (18a) with $F(Pr) = Pr^{-0.57}$

$$St = \frac{f/2}{1 + \sqrt{(f/2)} [\bar{g}(e^+) Pr^{0.57} - u_e^+(e^+, p/e)]} \quad (19)$$

The correlations for $u_e^+(e^+, p/e)$ (Fig. 9) and $\bar{g}(e^+)$ (Fig. 11) are used to compute the friction factor and Stanton number. The following procedure outlines the method for calculation of f and St :

1. Specify the roughness geometry ($e/D, p/e$), the fluid (Pr) and assume a value of e^+ .
2. Read $(p/e)^{-0.53} u_e^+(e^+, p/e)$ from Fig. 9 and calculate $u_e^+(e^+, p/e)$.
3. Calculate f from equation (4b).
4. Read $\bar{g}(e^+)$ from Fig. (11).
5. Compute St using equation (19).
6. Compute $Re = e^+ \sqrt{(2/f)/(e/D)}$.

The calculation method requires e^+ as the independent flow variable rather than Re . However, using the above procedure it is easy to compute the St, f and Re corresponding to several values of e^+ and then to draw a graph of

St and *f* vs. *Re*. In the fully rough region ($e^+ > 35$) the Stanton number and friction factor for $10 < p/e < 40$ can be represented by equations (20) and (21)†.

$$St = \frac{f/2}{1 + \sqrt{(f/2)} [4.5 (e^+)^{0.28} Pr^{0.57} - 0.95 (p/e)^{0.53}]} \tag{20}$$

$$\sqrt{(2/f)} = 2.5 \ln (D/2e) - 3.75 + 0.95 (p/e)^{0.53} \tag{21}$$

Similar, but more complex, equations may be written for *St* and *f* in the region $6 < e^+ < 35$. The $\bar{g}(e^+)$ may be represented by a polynomial in e^+ , but u_e^+ does not show a simple p/e dependency.

Comparison with other correlating methods

Additional confirmation of the heat-momentum analogy correlation is provided by comparing it with other methods frequently found in the literature. Figure 12 shows the present results for air plotted in the form St/St_s vs. e^+ . This correlation is not very good, although the data for the geometrically similar roughnesses are correlated within ± 11 per cent. These results are poorer than found by Sheriff and Gumley [21] and Sutherland [22], whose

repeated-rib air data for $10 < p/e < 15$ were correlated within ± 5 per cent.

Figure 13 shows the data for $Pr = 0.71$ and 21.7 correlated in the form η vs. e_{sg}^+ as proposed

by Burck [11]. With the exception of the roughest tube (04/10), the air data are well correlated by this method. However, the cor-

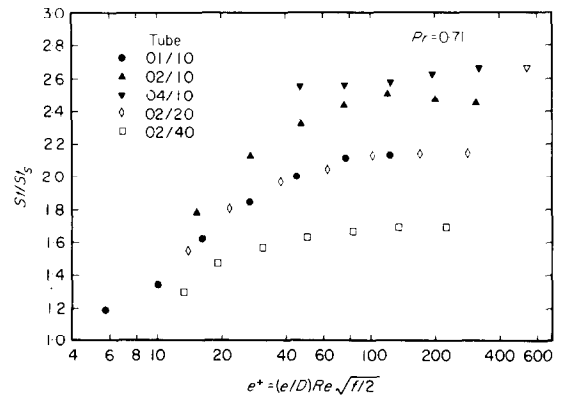


FIG. 12. St/St_s vs. e^+ for $Pr = 0.71$.

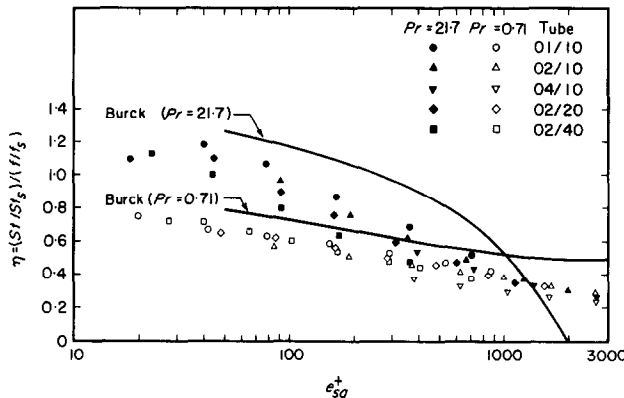


FIG. 13. η vs. e_{sg}^+ for $Pr = 0.71$ and 21.7 and comparison with Burck's [8] correlation.

† The constant 4.5 in equation (20) differs slightly from that given in [27], which used 4.75.

relation for the $Pr = 21.7$ data is noticeably poorer. The solid lines show the empirical

function $\eta(e_{sg}^+, Pr)$ proposed by Burck, which apparently fails for $e_{sg}^+ > 1000$. Burck shows a substantially larger effect of Prandtl number on η than found in this study.

Edwards [30] correlated his repeated-rib air data with the heat-momentum analogy method, but he used $u_e^+(e_{sg}^+)$ and e_{sg}^+ rather than $u_e^+(e^+, p/e)$

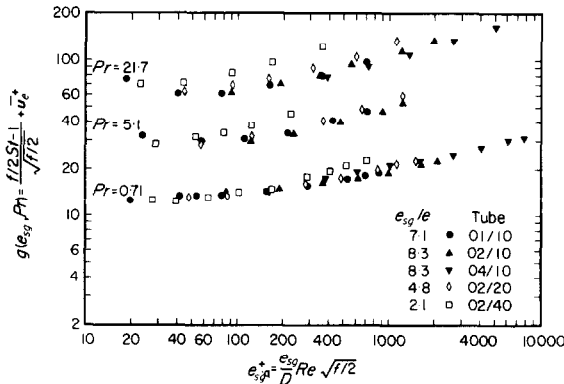


FIG. 14. Heat-momentum analogy correlation using equivalent sand-grain roughness.

and e^+ . Figure 14 shows the data of the present study correlated in the form used by Edwards. The $Pr = 0.71$ data are correlated about as well as on Fig. 10 except that the data for tube 02/40 show a measurable deviation at the highest e_{sg}^+ ; the deviation is even more pronounced at the higher Prandtl number. The reason for the poorer correlation is easily explained. Translation of the correlation from the e^+ plane to the e_{sg}^+ plane shifts the data relatively by e_{sg}^+/e^+ along the abscissa and by $[u_e^+(e_{sg}^+) - u_e^+(e^+, p/e)]$ along the ordinate. The vertical shift is nearly

insignificant at the higher Prandtl numbers, especially for $p/e = 40$. Values of e_{sg}/e for the fully rough condition are tabulated on Fig. 14 and show that the geometrically similar roughness data have received about the same shift. However, the data for tubes 02/20 and 02/40 have been shifted only 60 per cent and 25 per cent as much, respectively. Therefore, only geometrically similar roughness data will be correlated equally well by both methods. A correlation based on $\bar{g}(e_{sg}^+)$ would have a different exponent on the Prandtl number function than the $\bar{g}(e^+)$ correlation of Fig. 11.

The effect of Prandtl number

Perhaps the least understood aspect of rough surfaces is the influence of the Prandtl number. The Prandtl number influence may be evaluated by examining the behavior of the variable $\eta \equiv (St/St_s)/(f/f_s)$. If the effect of Prandtl number on the Stanton were the same for rough and smooth tubes, η (or St/St_s) would be independent of Prandtl number. This η parameter may also be described as an "efficiency index", since it defines the relative friction expenditure (f/f_s) necessary to yield a given heat transfer augmentation (St/St_s) for equal Reynolds number. An equation for η results by substituting equations (15) and (19) in the equation which defines η .

$$\eta = \frac{1 + 9.3\sqrt{(f_s/2)}(Pr - 1)Pr^{-\frac{1}{2}}}{1 + \sqrt{(f/2)}(\bar{g}Pr^{0.57} - u_e^+)}. \quad (22)$$

Using equation (4b) for $\sqrt{(2/f)}$ and the Blasius friction factor for $\sqrt{(f_s/2)}$, which is defined in terms of e^+ , equation (22) becomes

$$\eta = \frac{1 + \frac{9.3\sqrt{(a/2)}(Pr - 1)Pr^{-\frac{1}{2}}}{\{e^+[u_e^+(e^+, p/e) - 3.75 - 2.5 \ln(2e/D)]\}^{b/2}}}{1 + \frac{\bar{g}(e^+)Pr^{0.57} - u_e^+(e^+, p/e)}{u_e^+(e^+, p/e) - 3.75 - 2.5 \ln(2e/D)}} \quad (23)$$

where the constants a and b apply to the Blasius friction factor ($a = 0.079$, $b = 0.25$ for $Re < 50000$ and $a = 0.046$, $b = 0.20$ for $Re > 50000$).

Equation (23) has the functional form $\eta = \eta(e^+, p/e, e/D, Pr)$, which is graphically portrayed on Fig. 15 for $p/e = 10$. The lower portion of Fig. 15 shows the influence of Pr on η for $e/D = 0.01$. The Prandtl number dependency of rough tubes is about equal to that of smooth tubes for $e^+ > 250$. However, for $e^+ < 250$ the rough tube Prandtl number dependency differs substantially from that of smooth tubes. The upper portion of Fig. 15 shows the degree to which η is also influenced by e/D .

The results shown in Fig. 15 differ from the conclusions of Kalinin [7] and Burck [11].

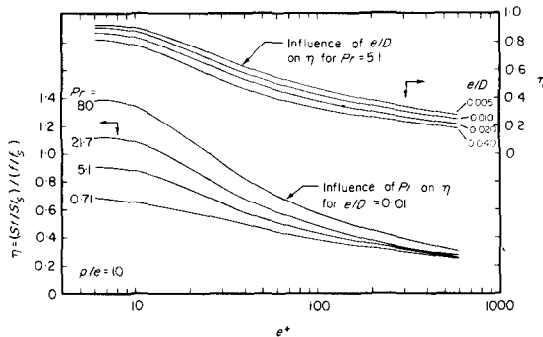


FIG. 15. The influence of Pr and e/D on η vs. e^+ , for $p/e = 10$, calculated from equation (23).

Kalinin found that η is essentially independent of Prandtl number, which agrees with this work only for $e^+ > 250$. Burck argues that all roughness geometries have the same curves of $\eta(e_{sg}^+, Pr)$ and concludes a negligible dependency of η on e/D . Except for the e/D dependency, Burck's conclusions are in qualitative agreement with this work only for $e^+ < 250$ (or $e_{sg}^+ < 1000$).

A comparison of this data with other existing repeated-rib data, as well as other roughness types, will be presented in a future publication. A quantitative criterion for selection of the e/D , which yields a high value of η and St/St_s at any arbitrary Reynolds number, will also be given in this paper.

CONCLUSIONS

1. Repeated-rib friction data are well correlated (Fig. 9) using law of the wall similarity with a logarithmic velocity distribution.
2. The heat-momentum transfer analogy, based on law of the wall similarity, adequately correlates the repeated-rib heat transfer data over a wide range of e/D , p/e and Pr (Fig. 11). This correlation is found to be superior to other methods, especially in accounting for the effect of Prandtl number.
3. The heat transfer and friction correlations may be extended to a wider range of e/D by virtue of law of the wall similarity. The correlations specifically apply to ribs of rectangular cross-section, whose thickness is small relative to the rib spacing.
4. This work and the prior studies of Nikuradse, and Dipprey and Sabersky offer strong arguments for application of law of the wall similarity and heat-momentum analogy correlating methods to geometrically similar forms of arbitrary roughness.
5. The results of this study argue against a single correlation for all roughness geometries, as proposed by Burck.

REFERENCES

1. W. NUNNER, Heat transfer and pressure drop in rough pipes, *VDI-Forsch.* **22**, 455B (1959). English trans., AERE Lib./Trans. 786 (1958).
2. R. KOCH, Pressure loss and heat transfer for turbulent flow, *VDI-Forsch.* **29**, 469B (1958). English trans., AEC-tr-3875 (1960).
3. J. GARGAUD and G. PAUMARD, Amelioration du transfert de chaleur par l'emploi de surfaces corrugées, Commissariat à l'énergie Atomique, Report CEA-R 2464 (1964).
4. J. MOLLOY, Rough tube friction factors and heat transfer coefficients in laminar and transition flow, UKAEA AERE-R5415 (1967).
5. W. A. SUTHERLAND and C. W. MILLER, Heat transfer to superheated steam—II, improved performance with turbulence promoters, USAEC Report, GEAP-4749 (1964).
6. E. C. BROUILLETTE, T. L. MIFFLIN and J. E. MYERS, Heat transfer and pressure drop characteristics at internal finned tubes, ASME Paper 57-A-47, presented at ASME Annual Meeting, New York (Dec. 1957).
7. E. K. KALININ, G. A. DREISTLER and S. A. YARKHO, Experimental study of heat transfer intensification

- under condition of forced flow in channels, JSME Semi-International Symp., paper 210 (1967).
8. E. W. SAMS, Experimental investigation of average heat transfer and friction coefficients for air flowing in circular pipes having square-thread type roughness, NACA RM-E 52D17 (1952).
 9. V. GOMELAURI, Influence of two-dimensional artificial roughness on convective heat transfer, *Int. J. Heat Mass Transfer* **7**, 653-663 (1964).
 10. V. KOLAR, Heat transfer in turbulent flow of fluids through smooth and rough tubes, *Int. J. Heat Mass Transfer* **8**, 639-653 (1964).
 11. E. BURCK, Influence of Prandtl number on heat transfer and pressure drop of artificially roughened channels, *Wärme-u. Stoff.* **2**, 87-98 (1969).
 12. W. B. HALL, Heat transfer in channels having rough and smooth surfaces, *J. Mech. Engng Sci.* **4**, 287-291 (1962).
 13. F. J. EDWARDS and N. SHERIFF, The heat transfer and friction characteristics for forced convection air flow over a particular type of rough surface, *International Developments in Heat Transfer*. ASME, 415-425 (1961).
 14. W. H. EMERSON, Heat transfer in a duct in regions of separated flow, *Proc. Third Int. Heat Transfer Conf.* **1**, 267-275 (1966).
 15. T. J. MUELLER, On separation, re-attachment and redevelopment of turbulent boundary layers, Ph.D. Thesis, Univ. of Ill. (1961).
 16. C. K. LIU, S. J. KLINE and J. P. JOHNSTON, An experimental study of turbulent boundary layers on rough walls, Stanford Univ. Report MD-15, pp 547-553 (1966).
 17. T. UEDA and I. HARADA, Experiments of heat transfer on surfaces with transverse fins for flow direction, *Bull. JSME*, **7**, 759-768 (1964).
 18. J. G. KNUDSEN and D. L. KATZ, *Fluid Dynamics and Heat Transfer*, p. 197. McGraw-Hill, New York (1958).
 19. J. NIKURADSE, Laws of flow in rough pipes, *VDI Forsch.* 361 (1933). English translation, NACA TM-1292 (1965).
 20. D. F. DIPPREY and R. H. SABERSKY, Heat and momentum transfer in smooth and rough tubes at various Prandtl numbers, *Int. J. Heat Mass Transfer* **6**, 329-353 (1963).
 21. N. SHERIFF and P. GUMLEY, Heat transfer and friction properties of surfaces with discrete roughness, *Int. J. Heat Mass Transfer* **9**, 1297-1320 (1966).
 22. W. A. SUTHERLAND, Improved heat transfer performance with boundary layer turbulence promoters, *Int. J. Heat Mass Transfer* **10**, 1589-1599 (1967).
 23. J. C. ROTTA, Recent developments in calculation methods for turbulent boundary layers with pressure gradients and heat transfer, *J. Appl. Mech.* **88**, 429 (1966).
 24. E. R. G. ECKERT, Heat transfer—a lecture at the Osborne Reynolds Centenary Celebrations, Univ. of Manchester, England, to be published in the Celebration Proceedings (Oct. 1968).
 25. R. G. DEISSLER, Analysis of turbulent heat transfer, mass transfer and friction in smooth tubes at high Prandtl and Schmidt numbers, NACA Report 1210 (1955).
 26. E. M. SPARROW, T. M. HALLMAN and R. SIEGEL, Turbulent heat transfer in the thermal entrance region of a pipe with uniform heat flux, *Appl. Sci. Res.* **A7**, 37-52 (1957).
 27. R. L. WEBB, Turbulent heat transfer in tubes having two-dimensional roughness, including the effect of Prandtl number, Ph.D. Thesis, University of Minnesota (1969).
 28. W. HUFSCHMIDT, E. BURCK and W. RIEBOLD, Die Bestimmung Ortlicher und Mittlerer Wärmeübertragungszahlen in Rohren bei Hohen Warmestromdichten, *Int. J. Heat Mass Transfer* **7**, 539-565 (1966).
 29. D. BETTERMAN, Contribution à l'étude de la convection forcée turbulente le long de plaques rugueuses, *Int. J. Heat Mass Transfer* **9**, 153-164 (1966).
 30. F. J. EDWARDS, The correlation of forced convection heat transfer data from rough surfaces in ducts having different shapes of flow cross-section, *Proc. Third Int. Heat Transfer Conf.* **1**, 32-44 (1966).
 31. J. O. HINZE, Turbulent pipe flow, *The Mechanics of Turbulence*, pp. 129-165. Gordon & Breach, New York (1961).

TRANSFERT THERMIQUE ET FROTTEMENT DANS DES TUBES À RUGOSITÉ ANNULAIRE RÉPÉTÉE

Résumé—On développe des corrélations de transfert thermique et de frottement pour un écoulement turbulent dans des tubes ayant une rugosité annulaire répétée. La corrélation de frottement est basée sur la loi de similitude de la paroi qui est la même méthode qu'utilise Nikuradse pour la rugosité des grains de sable. La corrélation de transfert thermique appliquée à un écoulement sur une surface rugueuse l'analogie de transfert chaleur-quantité de mouvement qui a d'abord été utilisée par Dipprey et Sabersky pour la rugosité de grains de sable. Les corrélations sont vérifiées à l'aide des résultats expérimentaux relatifs à $0,01 < e/D < 0,04$ et $10 < p/e < 40$ et couvrant le domaine $0,71 < Pr < 37,6$. Les corrélations peuvent être étendues à un domaine plus large du rapport e/D en vertu de la loi de la paroi. Les bons résultats obtenus dans cette étude, renforcés par l'étude antérieure de la rugosité des grains de sable, offrent un argument important pour l'application de méthodes corrélatives à d'autres géométries de rugosité. Le succès de l'analogie chaleur-quantité de mouvement est comparé à d'autres méthodes fréquemment trouvées dans la littérature.

WÄRMEÜBERGANG UND REIBUNG IN ROHREN MIT RIPPENFÖRMIGEN
RAUHIGKEITEN

Zusammenfassung—Für turbulente Strömung in Rohren mit rippenförmigen Rauigkeiten wurden Beziehungen für den Wärmeübergang und die Reibung aufgestellt. Die Reibungsbeziehung ist aufgebaut auf dem Wandähnlichkeitsgesetz nach derselben Methode, die Nikuradse für Sandkornrauigkeit verwendete. Die Wärmeübergangsbeziehung basiert auf der Anwendung einer Wärme-Impulsübertragungsanalogie für die Strömung über raue Oberflächen, die zuerst von Dippyrey und Sabersky für Sandkornrauigkeit benutzt wurde. Die Beziehungen wurden verwirklicht mit Versuchsergebnissen für $0,01 < e/D < 0,04$ und $10 < p/e < 40$ im Bereich $0,71 < Pr < 27,6$. Die Beziehungen können dank des Wandgesetzes auch auf einen grösseren Bereich von e/D angewandt werden. Die guten Ergebnisse in dieser Arbeit, die auch durch frühere Arbeiten über Sandkornrauigkeit unterstützt werden, sprechen stark für Anwendung der Korrelationsmethoden auf andere Rauigkeitsgeometrien. Die Analogiebeziehung zwischen Wärme- und Impulsübertragung wird mit anderen Methoden verglichen, die sich häufig in der Literatur finden.

ТЕПЛООБМЕН И ТРЕНИЕ В ТРУБАХ С РАВНОМЕРНОЙ
ШЕРОХОВАТОСТЬЮ

Аннотация—Разработаны обобщающие соотношения по теплообмену и трению для турбулентного потока в трубах с равномерной шероховатостью. В основу соотношения по трению лег закон подобия стенок и метод, использованный Никурадзе для шероховатости песка. Соотношение по теплообмену основано на применении аналогии переноса тепла и количества движения к потоку на шероховатой поверхности, впервые примененной Диппреем и Саберским для шероховатости песка. Соотношения подтверждаются экспериментальными Данными, взятыми для $0,01 < e/D < 0,04$ и $10 < p/e < 40$ в диапазоне $0,71 < Pr < 37,6$. Благодаря закону стенки обобщающие соотношения могут быть расширены до более широкого диапазона e/D . Хорошие результаты, полученные при этом исследовании и подкрепленные предыдущей работой по шероховатости песка, свидетельствуют в пользу применения корреляционных методов к другим шероховатым геометриям. Результативность корреляции по аналогии переноса тепла и количества движения сравнивается с другими методами, часто встречающимися в литературе.